

Desorption Electrospray Ionization Mass Spectrometry Imaging of Proteins Directly from Biological Tissue Sections

Kyana Y. Garza, Clara Leigh Feider, Dustin R Klein, Jake
A. Rosenberg, Jennifer S. Brodbelt, and Livia S. Eberlin

Anal. Chem., **Just Accepted Manuscript** • DOI: 10.1021/acs.analchem.8b00967 • Publication Date (Web): 25 May 2018

Downloaded from <http://pubs.acs.org> on May 25, 2018

Just Accepted

“Just Accepted” manuscripts have been peer-reviewed and accepted for publication. They are posted online prior to technical editing, formatting for publication and author proofing. The American Chemical Society provides “Just Accepted” as a service to the research community to expedite the dissemination of scientific material as soon as possible after acceptance. “Just Accepted” manuscripts appear in full in PDF format accompanied by an HTML abstract. “Just Accepted” manuscripts have been fully peer reviewed, but should not be considered the official version of record. They are citable by the Digital Object Identifier (DOI®). “Just Accepted” is an optional service offered to authors. Therefore, the “Just Accepted” Web site may not include all articles that will be published in the journal. After a manuscript is technically edited and formatted, it will be removed from the “Just Accepted” Web site and published as an ASAP article. Note that technical editing may introduce minor changes to the manuscript text and/or graphics which could affect content, and all legal disclaimers and ethical guidelines that apply to the journal pertain. ACS cannot be held responsible for errors or consequences arising from the use of information contained in these “Just Accepted” manuscripts.



1
2
3 **Desorption Electrospray Ionization Mass Spectrometry Imaging of Proteins Directly from**
4
5 **Biological Tissue Sections**
6

7 Kyana Y. Garza, Clara L. Feider, Dustin R. Klein, Jake A. Rosenberg, Jennifer S. Brodbelt, and
8
9 Livia S. Eberlin*
10

11
12
13 Department of Chemistry, The University of Texas at Austin, Austin, TX, 78712
14

15 * to whom correspondence should be addressed: liviase@utexas.edu
16
17
18
19
20
21

22 **Abstract**
23

24 Analysis of large biomolecules including proteins has proven challenging using ambient
25 ionization mass spectrometry imaging techniques. Here, we have successfully optimized
26 desorption electrospray ionization mass spectrometry (DESI-MS) to detect intact proteins
27 directly from tissue sections, and further integrated DESI-MS to a high field asymmetric
28 waveform ion mobility (FAIMS) device for protein imaging. Optimized DESI-FAIMS-MS
29 parameters were used to image mouse kidney, mouse brain, and human ovarian and breast
30 tissue samples, allowing detection of 11, 16, 14, and 16 proteoforms, respectively. Identification
31 of protein species detected by DESI-MS was performed on-tissue by top-down ultraviolet
32 photodissociation (UVPD) and collision induced dissociation (CID), as well as using tissue
33 extracts by bottom-up CID and top-down UVPD. Our results demonstrate that DESI-MS imaging
34 is suitable for the analysis of the distribution of proteins within biological tissue sections.
35
36
37
38
39
40
41
42
43
44
45
46
47
48
49
50

51 Mass spectrometry (MS) imaging is a powerful tool to investigate the spatial distribution
52 of molecular species directly from tissue samples.^{1,2} Matrix assisted laser desorption/ionization
53 (MALDI) is the most widely used MS imaging technique, which has been extensively explored to
54
55
56
57
58
59
60

1
2
3 image and characterize metabolites, lipids, and proteins from biological tissue sections.^{1,3}
4
5 Ambient ionization MS techniques have become increasingly used for biological tissue imaging
6
7 as they allow analysis to be performed in the open environment with minimal sample
8
9 preparation requirements, which is appealing for clinical applications.^{2,4} Desorption electrospray
10
11 ionization (DESI) MS imaging, for example, is the most widely used ambient ionization MS
12
13 technique that has been broadly explored tissue imaging.⁴
14
15

16 DESI-MS imaging has been successfully used to analyze biological tissue sections
17
18 allowing efficient desorption and ionization of lipids and metabolites that are diagnostic of
19
20 cancer including breast,⁵ ovarian,⁶ brain,⁷ and others⁴. Although typically used for small
21
22 molecule analysis, a few studies have described optimization of DESI-MS for protein analysis
23
24 from non-biological substrates.⁸⁻¹⁰ For example, DESI-MS has been recently used to desorb
25
26 membrane proteins in their native conformations from planar surfaces.¹⁰ However, inefficient
27
28 desorption of large biomolecules and chemical noise arising from the complex tissue matrix
29
30 have impeded detection of proteins directly from biological tissue sections by DESI-MS.
31
32 Recently, ambient ionization MS using liquid extraction techniques such as nanospray
33
34 desorption electrospray ionization (nano-DESI),¹¹ liquid extraction surface analysis (LESA),¹²
35
36 and the liquid microjunction surface sampling probe (LMJ-SSP)¹³ were applied to image
37
38 proteins from biological tissue sections. In the latter two studies, protein analysis was enhanced
39
40 by integrating ion mobility separation into the workflow, which allowed selected transmission of
41
42 protein ions and reduced chemical noise in the mass spectra.^{12,13} Here, we describe the
43
44 optimization of DESI-MS imaging for protein analysis and further coupling of DESI to a FAIMS
45
46 device for imaging proteins from biological tissue sections, indicating that this approach could
47
48 be used for top-down proteomics studies in various biomedical applications.
49
50

51 We first evaluated the effectiveness of a washing step with organic solvents on
52
53 enhancing protein detection, which is commonly performed in MALDI-MS imaging experiments
54
55 to remove endogenous lipids and biological salts that may affect efficiency of protein desorption
56
57
58
59
60

1
2
3 and ionization.¹⁴ Detailed methods are provided in the **Supporting Information**. DESI-MS
4
5 imaging was performed on an unwashed mouse kidney tissue section in the positive ion mode
6
7 using pure ACN as the solvent and typical DESI-MS lipid imaging parameters (**Table S1**).¹⁵ Ions
8
9 identified as triacylglycerols and glycerophosphocholines lipids were detected at high relative
10
11 abundances (**Figure 1a**),¹⁵ while multiply charged protein ions, were not seen. Next, a solvent
12
13 system of ACN:H₂O (80:20) (v/v) with 0.2% formic acid previously reported to enhance protein
14
15 desorption by nanoDESI was used for analysis of unwashed tissue sections, at a flow rate of 5
16
17 μ L/min.¹¹ Similar lipid species were detected at high relative abundances in addition to multiply
18
19 charged ions at low abundances that were tentatively identified as protein species (**Figure 1b**).
20
21 The lipid washing step was then performed on an adjacent mouse kidney tissue section
22
23 followed by DESI-MS imaging analysis at the same parameters (**Figure 1c**). While the washing
24
25 step was effective at removing lipids, the mass spectra obtained presented low total ion
26
27 abundance of the multiple charged ions. Previous studies have reported that the desorption of
28
29 protein standards from glass slides by DESI-MS is dependent on the spray angle and spray-to-
30
31 surface distance.^{10,16} Thus, we performed optimization of DESI spray parameters for protein
32
33 detection by tuning angle, spray-to-sample distance, and sample-to-inlet distance to 55°, 3.5
34
35 mm, and 2.5 mm, respectively. Performance was evaluated by the improvement in the total ion
36
37 abundance of m/z 938.117, later identified as an alpha-globin proteoform with an asparagine to
38
39 a lysine substitution. While protein ions were detected in mouse kidney tissue at various spray-
40
41 to-sample and sample-to-inlet distances, proteins were not detected above a S/N=3 using spray
42
43 angles other than 55°, indicating that protein desorption and detection is more strongly
44
45 dependent on the spray angle than other source parameters. At these optimized parameters,
46
47 the alpha-globin proteoform was detected with S/N = 27.9 (average of n=3 tissue sections, n=3
48
49 lines/tissue section, n=20 mass spectra/line), as well as 10 other distinct protein species
50
51
52
53
54 (**Figure 1d**).
55
56
57
58
59
60

1
2
3 In an effort to further increase S/N of proteins, we integrated FAIMS to the DESI-MS
4 imaging source and mass spectrometer interface as we have previously described.¹³ Two-
5 dimensional FAIMS sweep experiments were performed to determine the optimal dispersion
6 field (DF = 180 Td) and compensation field (CF = +1.0 Td) for protein detection. Under the
7 optimized FAIMS parameters, a S/N=32.1 was achieved for the alpha-globin proteoform
8 (average of n=3 tissue sections, n=3 lines/tissue section, n=20 mass spectra/line), as well as
9 detection of 10 other distinct protein species (**Table S2 and Figure 1e**). The addition of FAIMS
10 increased the S/N for all the proteins detected, thus improving image contrast and quality
11 (**Figure S1**). The increase in the S/N of protein ions was due to the substantial filtering of
12 interfering background species (68% decrease), including abundant solvent peaks, and
13 reduction of chemical noise (43% decrease), despite an overall drop (30%) in the absolute
14 intensities of protein ions (**Figure S2**). Therefore, all further experiments were performed using
15 the optimized FAIMS parameters. Spray voltage and transfer capillary temperature were also
16 tuned to optimal values of 1 kV and 300°C for protein detection, respectively, using the
17 optimized DESI-FAIMS parameters (**Figure S3 and Figure S4**). For more details on the effect
18 of FAIMS in the data and the optimization approach, please see the **Supporting Information**.

19
20
21
22
23
24
25
26
27
28
29
30
31
32
33
34
35
36
37 Top-down and bottom-up protein-sequencing methods were explored to identify the
38 proteins detected. On-tissue CID was performed online by isolating and fragmenting protein
39 ions while directly profiling the tissue sections using DESI-MS alone (no FAIMS). Fragmentation
40 of the 13+ charge state isotope envelope of the ion at m/z 1,153.298 (MM = 15,085 Da, **Figure**
41 **S5**) by CID allowed identification of this ion as the alpha globin protein (16% sequence
42 coverage) in mouse kidney tissue section. Other proteoforms of alpha-globin were detected at
43 high relative abundances, which are likely associated to the highly vascularized nature of the
44 kidney tissue. In an effort to obtain higher sequence coverage, UVPD was integrated with
45 DESI-MS for on-tissue protein fragmentation (no FAIMS).¹⁷ The proteoform of alpha-globin
46 presenting an asparagine to a lysine substitution (MM = 14,985 Da) used for optimization was
47
48
49
50
51
52
53
54
55
56
57
58
59
60

1
2
3 identified by on-tissue UVPD of m/z 938.114 (16+ charge state, 32% sequence coverage)
4
5 (**Figure 1f** and **Figure S6**). Hemoglobin α (m/z 1009.335, 15+ charge state) was identified from
6
7 normal human ovarian tissue using on-tissue UVPD (sequence coverage of 20%). These results
8
9 demonstrate feasibility of UVPD for the identification of abundant proteins detected using DESI-
10
11 MS from biological tissue sections, and to the best of our knowledge represent the first
12
13 application of UVPD for on-tissue protein identification. Nevertheless, further optimization of this
14
15 integrated approach is needed for fragmentation and identification of lower abundant protein
16
17 species. Top-down UVPD and bottom-up proteomics were also performed on protein extracts
18
19 obtained from the tissues analyzed to assist in the identification of low abundance protein ions.
20
21 Sequence coverage for the proteins identified and the respective method used are provided in
22
23 **Table S3**.

24
25
26 Next, we applied the optimized DESI-FAIMS approach to image proteins from biological
27
28 tissue sections. As shown in **Figure S7**, DESI-FAIMS allowed imaging of a variety of proteins
29
30 from mouse brain tissue sections at distinct spatial distributions within histologic structures.
31
32 These results were reproducible across multiple mouse brain tissue sections and in agreement
33
34 with what previously reported by nanoDESI and LMJ-SSP.^{11,13} Further, multimodal DESI
35
36 imaging was performed to obtain both lipid and protein information from the same mouse brain
37
38 tissue section. For more information on mouse brain tissue imaging, please see **Supporting**
39
40 **Information and Figures S8, S9 and S10**.

41
42
43 We next employed DESI-FAIMS to image proteins from human normal and cancer
44
45 tissue sections. As shown in **Figure 2a**, the mass spectra obtained from normal ovarian and
46
47 high-grade serous ovarian cancer (HGSC) tissue sections showed distinct relative abundances
48
49 of protein ions. Hemoglobin β (m/z 1443.318; 11+ charge state; MM = 15,998 Da), for example,
50
51 was observed at high relative abundances in healthy ovarian tissue samples, while the S100A6
52
53 protein (m/z 1442.339; 7+ charge state; MM = 10,180 Da), was observed at high relative
54
55 abundances in HGSC tissue. Note that although differing by ~ 1 m/z value, hemoglobin β and
56
57

1
2
3 S100A6 were clearly resolved in the mass spectra (**Figure 2b**) and identified using a top-down
4 approach. Increased abundance of S100A6 has been previously reported in a variety human
5 cancers.¹⁸ DESI-FAIMS ion images enabled clear visualization of protein ions within the
6 heterogeneous regions of a single tissue sample (**Figure 2c**), which corroborates with previous
7 findings.^{13,19}
8
9
10
11
12

13
14 DESI-FAIMS-MS imaging also allowed detection of several proteins from human normal
15 and a Her2- breast ductal breast carcinoma samples (**Figure 3**). For example, profilin-1 at m/z
16 1,152.460 (13+ charge state, MM = 15,054 Da) and hemoglobin α at m/z 1,009.536 (15+ charge
17 state) were observed at higher relative abundance in a normal breast tissue. On the other hand,
18 S100 proteins including S100A4 at m/z 1058.893 (11+ charge state, MM = 11,279 Da), S100A8
19 at m/z 986.633 (11+ charge state, MM = 10,835 Da), and S100A11 at m/z 1,166.091 (10+
20 charge state, MM = 11,740 Da), were seen at higher relative abundances in breast cancer
21 tissue (**Figure 3b**). Upregulation of members of the S100 family of proteins is known to occur in
22 breast cancer and has been reported by MALDI-MS imaging and other techniques.²⁰⁻²² Galectin-
23 1 (m/z 1,126.177, 13+ charge state, MM = 14,716 Da), previously associated with Her2- breast
24 cancer stromal tissue,²³ was also detected by DESI-FAIMS-MS at higher relative abundances in
25 the Her2- cancer tissue analyzed.
26
27
28
29
30
31
32
33
34
35
36
37
38

39 In conclusion, we describe the successful optimization of DESI for protein detection and
40 further coupling to a FAIMS device for protein imaging directly from biological tissue sections.
41 Addition of FAIMS at parameters optimized for protein transmission reduced the mass spectra
42 noise and transmission of background ions, resulting in higher S/N of protein ions and thus
43 improved imaging contrast and quality. We further demonstrate on-tissue top-down protein
44 identification using UVPD and CID for identification of abundant protein ions detected by DESI-
45 MS. While this study shows a noteworthy advancement for DESI-MS imaging, it represents an
46 initial step towards in-depth tissue proteomics applications. Most protein species detected are
47 highly abundant in biological tissues, such as hemoglobin and S100 proteins. Thus, additional
48
49
50
51
52
53
54
55
56
57
58
59
60

1
2
3 optimization is needed to improve the desorption efficiency of lower abundant proteins. Although
4 protein coverage by DESI-MS imaging remains vastly poorer to the coverage achieved through
5 traditional LC-MS/MS of tissue extracts and MALDI-MS imaging workflows,^{24,25} the ability to
6 rapidly image intact proteins from tissue sections with minimal sample preparation and under
7 ambient conditions suggests DESI-MS as a promising tool for top-down proteomics, with
8 potential applications in cancer imaging and diagnosis.
9
10
11
12
13
14
15
16
17

18 **Supporting Information**

19
20 Detailed materials, methods, and supporting results are described. Tables presenting DESI-MS
21 parameters, DESI-FAIMS S/N comparison, summary of detected and identified proteins, and
22 DESI-FAIMS optimization data are provided. Figures showing DESI mass spectra at various
23 optimization parameters, protein images of mouse brain with and without FAIMS, DESI mass
24 spectra of kidney tissue with and without FAIMS, voltage and temperature optimization mass
25 spectra, replicates of DESI-MS imaging, and MS/MS data of proteins are also included. The
26 supporting information is available free of charge via the Internet at <http://pubs.acs.org>.
27
28
29
30
31
32
33
34
35
36

37 **Acknowledgments**

38
39 This work was supported by The Welch Foundation (grant F-1895 LSE and F-1155 JSB) and
40 the National Institutes of Health (R00CA190783 to LSE and R21CA191664 to JSB). Tissue
41 samples were provided by the Cooperative Human Tissue Network (supported by the NCI), the
42 MD Anderson Cancer Center Tissue Bank. We thank Dr. Chandandeep Nagi and Dr. Jinsong
43 Liu for pathological evaluation, the University of Texas Proteomics Facility (funded by UT
44 System) for protein identification experiments and Marta Sans for assistance with experiments.
45
46
47
48
49
50
51
52
53

54 **Figures**

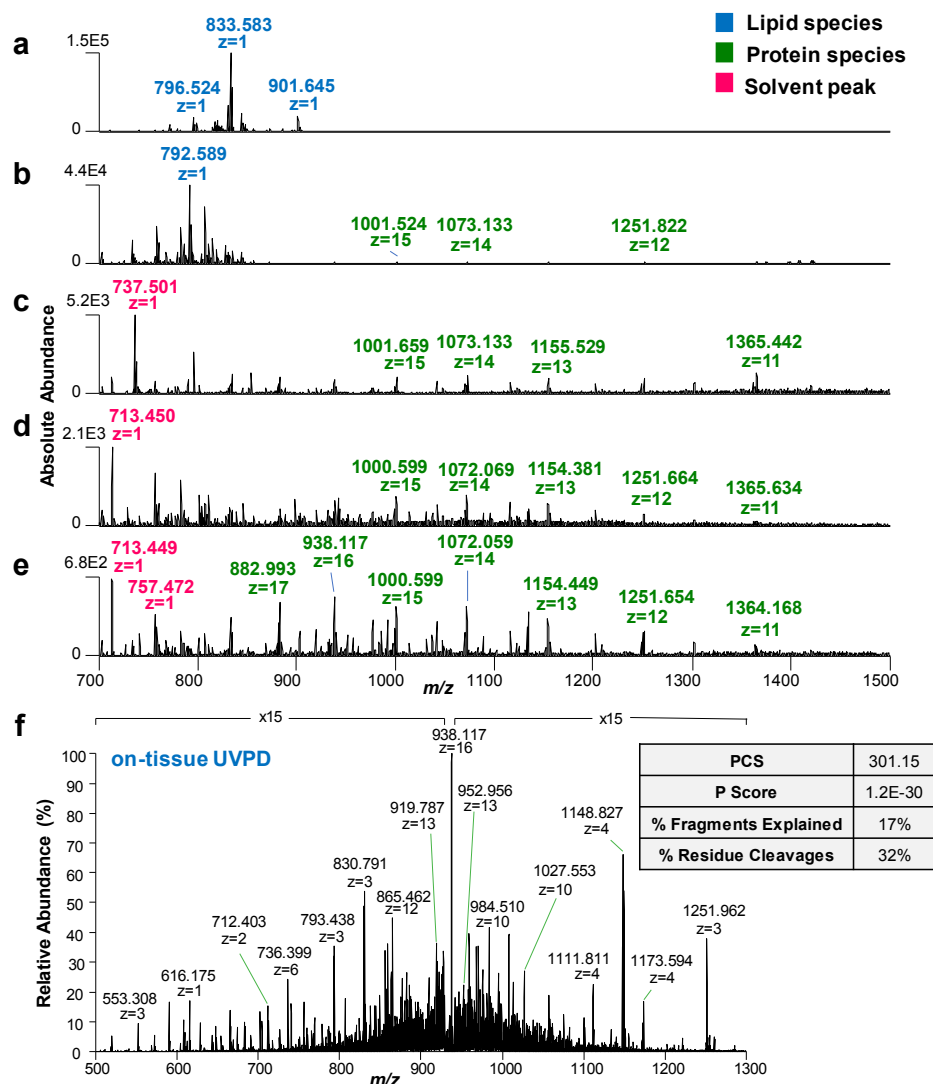


Figure 1. Representative positive ion mode DESI mass spectra obtained from mouse kidney tissue sections that were **a)** unwashed, using lipid DESI-MS parameters and pure ACN as solvent system, **b)** unwashed, using lipid DESI-MS parameters with ACN:H₂O 80:20 (v/v) and 0.2% formic acid as the solvent, **c)** washed, using lipid DESI-MS parameters and ACN:H₂O 80:20 (v/v) with 0.2% formic acid as the solvent, **d)** washed, using protein DESI-MS parameters and ACN:H₂O 80:20 (v/v) with 0.2% formic acid as the solvent, and **e)** washed, using protein DESI-FAIMS-MS parameters and ACN:H₂O 80:20 (v/v) with 0.2% formic acid as the solvent. Mass spectra are an average of 25 scans. **f)** On-tissue UVPD mass spectrum of m/z 938.117

from a mouse kidney tissue section (average of $n=80$ mass spectra). PCS, P-score, and sequence coverage are reported for the protein ion identified as an alpha-globin proteoform.

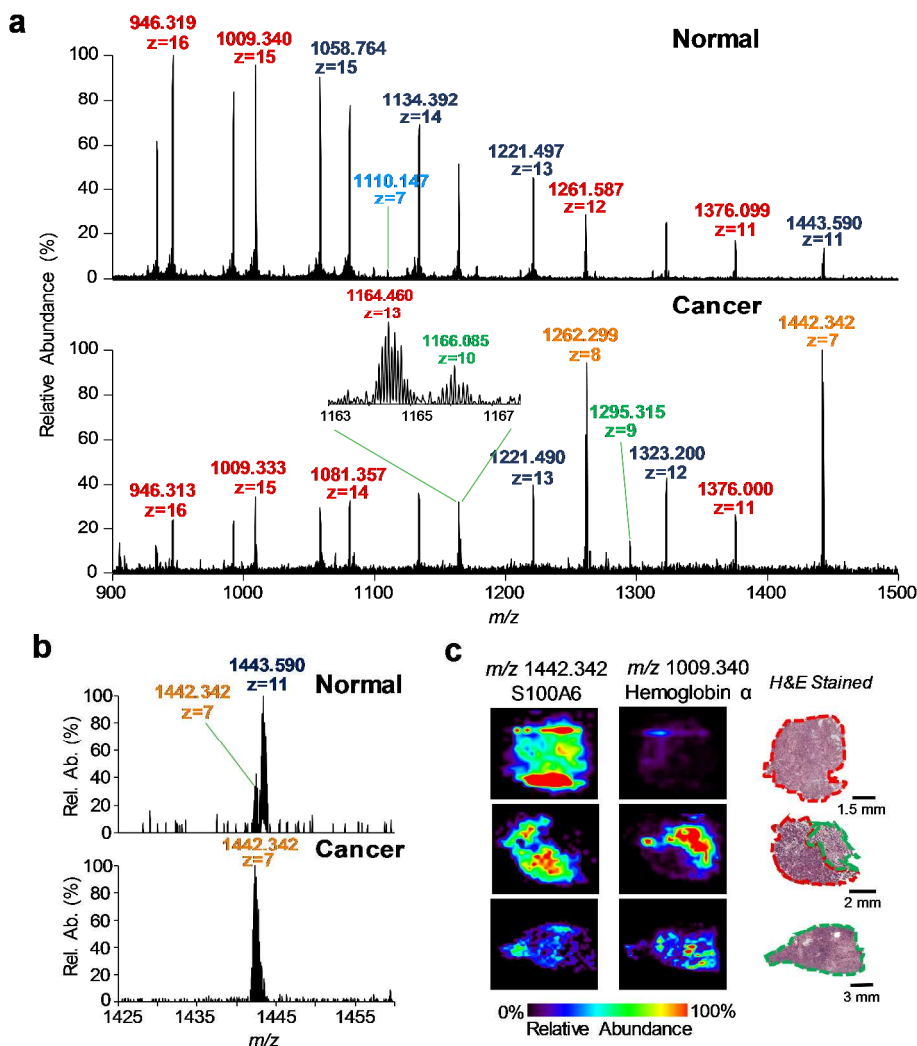
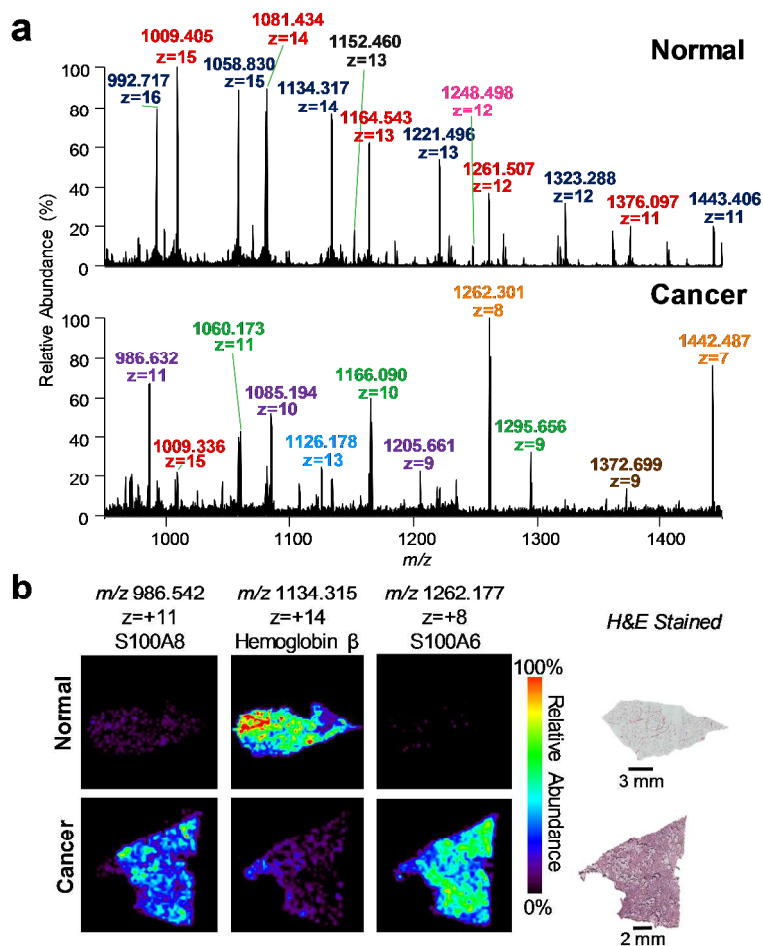


Figure 2. (a) Representative protein DESI-MS spectra of normal and HGSC ovarian tumor with optimized FAIMS parameters. Mass spectra are averages of 10 scans. Different charge states of the same protein species are denoted by same colored labels. (b) Zoomed in mass spectra of normal and HGSC samples, highlighting the observance of m/z 1442.339, identified as S100A6, within the cancer tissue. (c) DESI-MS ion images obtained from normal, pure cancer, and mixed normal/cancer ovarian tissue sections. Ion images are in the same scale. H&E

1
2
3 stained images are of a serial ovarian tissue sections as protein conditions are not histologically
4 compatible.
5
6
7
8
9
10
11

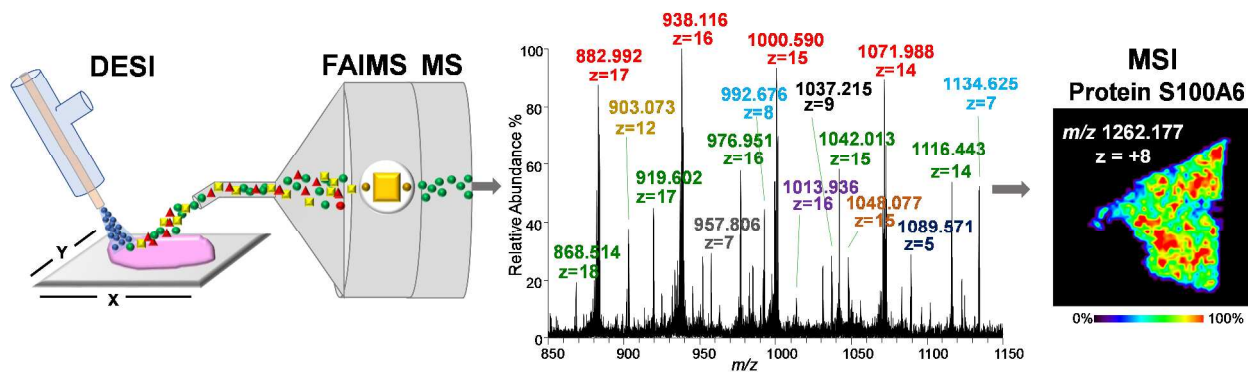


30
31
32
33
34
35
36
37
38
39
40
41
42
43 **Figure 3.** (a) Representative protein DESI-MS spectra of normal and breast cancer samples
44 with optimized FAIMS parameters. Mass spectra are averages of 20 scans. Different charge
45 states of the same protein species are denoted by same colored labels. (b) DESI-MS ion
46 images obtained from normal and breast cancer tissue sections. Ion images are in the same
47 scale. H&E stained images are of a serial breast tissue sections as protein conditions are not
48 histologically compatible.
49
50
51
52
53
54
55
56
57
58
59
60

References

- (1) Schwamborn, K.; Caprioli, R. M. *Mol Oncol* **2010**, *4*, 529-538.
- (2) Wu, C.; Dill, A. L.; Eberlin, L. S.; Cooks, R. G.; Ifa, D. R. *Mass Spectrom Rev* **2013**, *32*, 218-243.
- (3) Kriegsmann, M.; Casadonte, R.; Kriegsmann, J.; Dienemann, H.; Schirmacher, P.; Kobarg, J. H.; Schwamborn, K.; Stenzinger, A.; Warth, A.; Weichert, W. *Molecular & Cellular Proteomics* **2016**, *15*, 3081-3089.
- (4) Ifa, D. R.; Eberlin, L. S. *Clin Chem* **2016**, *62*, 111-123.
- (5) Calligaris, D.; Caragacianu, D.; Liu, X.; Norton, I.; Thompson, C. J.; Richardson, A. L.; Golshan, M.; Easterling, M. L.; Santagata, S.; Dillon, D. A.; Jolesz, F. A.; Agar, N. Y. R. *P Natl Acad Sci USA* **2014**, *111*, 15184-15189.
- (6) Sans, M.; Gharpure, K.; Tibshirani, R.; Zhang, J.; Liang, L.; Liu, J.; Young, J. H.; Dood, R. L.; Sood, A. K.; Eberlin, L. S. *Cancer Research* **2017**, *in press*.
- (7) Jarmusch, A. K.; Pirro, V.; Baird, Z.; Hattab, E. M.; Cohen-Gadol, A. A.; Cooks, R. G. *P Natl Acad Sci USA* **2016**, *113*, 1486-1491.
- (8) Honarvar, E.; Venter, A. R. *J Am Soc Mass Spectrom* **2017**, *28*, 1109-1117.
- (9) Shin, Y. S.; Drolet, B.; Mayer, R.; Dolence, K.; Basile, F. *Anal Chem* **2007**, *79*, 3514-3518.
- (10) Ambrose, S.; Housden, N. G.; Gupta, K.; Fan, J.; White, P.; Yen, H. Y.; Marcoux, J.; Kleanthous, C.; Hopper, J. T. S.; Robinson, C. V. *Angew Chem Int Ed Engl* **2017**, *56*, 14463-14468.
- (11) Hsu, C. C.; Chou, P. T.; Zare, R. N. *Anal. Chem.* **2015**, *87*, 11171-11175.
- (12) Griffiths, R. L.; Creese, A. J.; Race, A. M.; Bunch, J.; Cooper, H. J. *Anal. Chem.* **2016**, *88*, 6758-6766.
- (13) Feider, C. L.; Elizondo, N.; Eberlin, L. S. *Anal. Chem.* **2016**, *88*, 11533-11541.
- (14) Seeley, E. H.; Oppenheimer, S. R.; Mi, D.; Chaurand, P.; Caprioli, R. M. *Journal of the American Society for Mass Spectrometry* **2008**, *19*, 1069-1077.
- (15) Eberlin, L. S.; Ferreira, C. R.; Dill, A. L.; Ifa, D. R.; Cooks, R. G. *Biochimica Et Biophysica Acta-Molecular and Cell Biology of Lipids* **2011**, *1811*, 946-960.
- (16) Takats, Z.; Wiseman, J. M.; Cooks, R. G. *J Mass Spectrom* **2005**, *40*, 1261-1275.
- (17) Klein, D. R.; Holden, D. D.; Brodbelt, J. S. *Analytical Chemistry* **2016**, *88*, 1044-1051.
- (18) Bresnick, A. R.; Weber, D. J.; Zimmer, D. B. *Nat Rev Cancer* **2015**, *15*, 96-109.
- (19) Delcourt, V.; Franck, J.; Leblanc, E.; Narducci, F.; Robin, Y. M.; Gimeno, J. P.; Quanico, J.; Wisztorski, M.; Kobeissy, F.; Jacques, J. F.; Roucou, X.; Salzet, M.; Fournier, I. *EBioMedicine* **2017**, *21*, 55-64.
- (20) Cross, S. S.; Hamdy, F. C.; Deloulme, J. C.; Rehman, I. *Histopathology* **2005**, *46*, 256-269.
- (21) McKiernan, E.; McDermott, E. W.; Evoy, D.; Crown, J.; Duffy, M. J. *Tumor Biol* **2011**, *32*, 441-450.
- (22) Sanders, M. E.; Dias, E. C.; Xu, B. J.; Mobley, J. A.; Billheimer, D.; Roder, H.; Grigorieva, J.; Dowsett, M.; Arteaga, C. L.; Caprioli, R. M. *J Proteome Res* **2008**, *7*, 1500-1507.
- (23) Grosset, A. A.; Labrie, M.; Vladiou, M. C.; Yousef, E. M.; Gaboury, L.; St-Pierre, Y. *Oncotarget* **2016**, *7*, 18183-18203.
- (24) Kompauer, M.; Heiles, S.; Spengler, B. *Nat Methods* **2017**, *14*, 90-96.
- (25) Palma, C. D.; Grassi, M. L.; Thome, C. H.; Ferreira, G. A.; Albuquerque, D.; Pinto, M. T.; Melo, F. U. F.; Kashima, S.; Covas, D. T.; Pitteri, S. J.; Faca, V. M. *Molecular & Cellular Proteomics* **2016**, *15*, 906-917.

TOC figure



1
2
3
4
5
6
7
8
9
10
11
12
13
14
15
16
17
18
19
20
21
22
23
24
25
26
27
28
29
30
31
32
33
34
35
36
37
38
39
40
41
42
43
44
45
46
47
48
49
50
51
52
53
54
55
56
57
58
59
60